Competing through altering the environment: A cross-diffusion population model coupled to transport-Darcy equations [1]

Gonzalo Galiano [2] and Julián Velasco

Dpto. de Matemáticas, Universidad de Oviedo, c/ Calvo Sotelo, 33007-Oviedo Spain

Abstract

We consider an evolution model describing the spatial population distribution of two salt tolerant plant species, such as mangroves, which are affected by inter- and intra-specific competition (Lotka-Volterra), population pressure (cross-diffusion) and environmental heterogeneity (environmental potential). The environmental potential and the Lotka-Volterra terms are assumed to depend on the salt concentration in the roots region, which may change as a result of mangroves ability for uptaking fresh water and leave the salt of the solution behind, in the saturated porous medium. Consequently, partial differential equations modelling the population dynamics on the surface are coupled with Darcy-transport equations modeling the salt and pressure-velocity distribution in the subsurface. We prove the existence of weak solutions of the coupled problem and provide a numerical discretization based on a stabilized mixed finite element method, which we use to numerically demonstrate the behaviour of the system.

Key words: Population dynamics, cross-diffusion, Darcy flow, mixed formulation, existence of solutions, ecology of mangrove.

1 Introduction

We present a model for analyzing the spatial distribution evolution of two plant populations which are affected by

[1] Supported by the Spanish MEC Project MTM-2007-65088
[2] Corresponding author. Phone:+34 985103343 Fax: +34 985103354
[3] galiano@uniovi.es, julian@uniovi.es

- competition for similar resources,
- population pressure, and
- environmental quality.

These conditionings are realized mathematically in the form of a time evolution drift-cross diffusion system of partial differential equations, introduced by Shigesada, Kawasaki and Teramoto [30]:

$$\partial_t n_i - \operatorname{div} J_i = f_i(n_1, n_2), \quad J_i = \nabla(c_i n_i + a_{i1} n_i n_1 + a_{i2} n_i n_2) + d_i n_i \nabla U, \quad (1)$$

for $i = 1, 2$, where n_i denotes population density, f_i is a competition Lotka-Volterra type function,

$$f_i(n_1, n_2) = (\alpha_i - \beta_{i1} n_1 - \beta_{i2} n_2) n_i, \quad \alpha_i, \beta_{ij} \geq 0 \quad i, j = 1, 2, \qquad (2)$$

and U is the environmental potential, modeling areas where the environmental conditions are more or less favorable [30,28]. This model has received much attention since its introduction due to the interesting spatial pattern formation of its solutions, refered to as *segregation*. These patterns do not arise in the linear diffusion model, i.e. for $a_{ij} = 0$, $i, j = 1, 2$, where, if in addition $d_i = 0$, then the steady state solutions are constants determined by the zeros of the Lotka-Volterra terms. These constant solutions correspond, in general terms, to two kind of competitions: weak, which implies coexistence, and strong which implies extinction of one population. Lou and Ni [24,25] analysed the steady state problem corresponding to (1) (with $d_i = 0$) and proved the existence of non-constant solutions for some parameter combinations including weak and strong competition. Their results seem to indicate that while the intensity of diffusion (c_i) and self-diffusion (a_{ii}) tend to suppress pattern formation, those of cross-diffusion (a_{12}, a_{21}) seem to help create segregation patterns.

Mangrove ecosystems are tropical or subtropical communities of mainly tree species of great ecological importance due to the role they play as habitat builders and shoreline stabilizers, among others, covering large areas throughout the world [32]. They tipically grow in saline coastal soils, or muds, which develop through a combination of two processes: mineral sediment deposition and organic matter accumulation. This soil structure in conjunction to the usual flatness of the area and the almost permanent sea water saturation of the soil due to the regular inundation by tides, when not prolonged periods of waterlogging [20], causes a poor soil draining and flushing of the intersticial water. One of the decisive mangrove capabilities and perhaps the reason for its comparative fitness to the coastal areas is their ability to exclude most of the salt from the water their roots extract from the sea-water saturated soil, [3]. Passioura et al. [29] provided an analytical approach to the mechanisms of soil salinization produced by mangroves and investigated the consequences of salt concentration increase on mangroves transpiration rate. In their work, later generalized in a serie of papers [11,17,12], the authors presented one-

dimensional (depth) steady state equations governing the flow of salt and uptake of water in the root zone, for one mangrove specie, assuming that there is an upper limit c_1 to the salt concentration at which roots can take up water, and that the rate of uptake of water is proportional to the difference between the local concentration c and the assumed upper limit c_1. The general time-dependent N-dimensional model [12] reads

$$c_t + \operatorname{div}(Rc\mathbf{q} - \nabla c) = 0, \tag{3}$$
$$\operatorname{div} \mathbf{q} + g(\cdot, c) = 0, \tag{4}$$
$$\mathbf{q} + \nabla p + c\mathbf{e}_z = 0, \tag{5}$$

where c is the salt concentration, $\mathbf{q}$ the water flow, p the pressure, R a Rayleigh number and g the mangroves water extraction function, see (14) for an example. Observe that while the domain of equations (3)-(5) is the subsurface saturated porous medium, the equations for the populations densities (1) are defined only on the surface of the porous medium. The details of the model are given in the next section.

Passioura et al. [29] already pointed out the interesting ecological implications of the soil salinization induced by mangroves. Quoting the authors, "Differences between species in strategies of water use (i.e. the way in which water use and water-use efficiency relate to growth) may affect the distribution of these species. Species with high transpiration rates may dominate well-flushed habitats [less saline] while those adapted to low transpiration rates may occupy poorly flushed intertidal areas [more saline]". In a related work, Su Yean Teh et al. [31] focused on the situation in which a severe disturbance, such as a heavy storm, may lead to an invasion of salt tolerant species, such as mangroves, in geographical areas previously occupied by salt intolerant species, such as hardwood hammock species. They base their model upon the dynamics between vegetation and soil salinity but have a different mathematical approach than ours, since space is discretized in a grid of cells where some time differential equations are solved with suitable cell transmission conditions.

The aim of this article is to provide a time-space model expressed in terms of partial differential equations relating the population densities and their particular abilities to modify the environment through soil salinization. The feedback between populations and environment takes place in three ways: (i) through the water extraction functions, g_i, which depend on the relative presence of roots of each specie in the subsurface and on their particular ability to uptake fresh water from the soil. (ii) Through the salt distribution, c, which determines the environmental potential ($U = U(c)$) directing, possibly with different strengths, both populations towards lower salinized regions. And (iii), through different growth rates and competing behaviour, captured by Lotka-Volterra functions f_i, due again to species' ability to extract fresh water from

the salinized soil, i.e., through the dependence $f_i = f_i(g_1, g_2)$.

Let us finally mention a related population model, the *evolution of conditional dispersal* model, introduced and developed in a series of papers by Lou et al., see [9,7,19] and the references therein, in which the system (1) is particularized with $a_{ij} = 0$, i.e., without cross-diffusion, and with $f_i(n_1, n_2) = (U - n_1 - n_2)n_i$, i.e., Lotka-Volterra terms depending on the (given and time independent) environmental potential, in a similar spirit that our water extraction dependent Lotka-Volterra functions. For this model, the authors are able to provide conditions on the coefficients of the equations under which stability of either positive or semi-trivial steady state solutions hold. Although the complexity of the model described in the present paper does not allow to extract this kind of detailed information, we have numerically observed similar phenomena than those described for the conditional dispersal.

The outline of the article is the following. In Section 2 we first present independently the population model which develops on the soil surface and the transport-Darcy model which governs the salt and water relations in the susbsurface (porous medium). We then couple both models and state the problem to be solved. In Section 3 we give appropriate mathematical assumptions on the model data and prove the existence of solutions of the coupled surface-subsurface model. In Section 4 we introduce a scheme to discretize the problem and show some numerical simulations.

2 The mathematical model

2.1 On the surface: population dynamics

We first rescale the problem by introducing new unknowns, $u_1 = a_{21}n_1$ and $u_2 = a_{12}n_2$, for which we assume $a_{12}, a_{21} \neq 0$ in (1), i.e. the cross diffusion terms do not vanish. On the contrary, the model is much simpler, see [15]. These biomass densities, $u_i(x, y, t)$, are defined for the horizontal space variables $(x, y) \in \Gamma_D$, with $\Gamma_D \subset \mathbb{R}^2$ open and bounded and for $t \in (0, T)$ the time, for an arbitrarily fixed $T > 0$. The rescaled equations read [30]

$$\partial_t u_i - \operatorname{div} J_i = \tilde{F}_i(\cdot, u_1, u_2), \quad J_i = \nabla(c_i u_i + a_i u_i^2 + u_1 u_2) + d_i u_i \nabla U, \qquad (6)$$

in $S_T = \Gamma_D \times (0, T)$. Here, $\operatorname{div} = \frac{\partial}{\partial x} + \frac{\partial}{\partial y}$ and $\nabla = (\frac{\partial}{\partial x}, \frac{\partial}{\partial y})$.

The diffusion coefficients c_i and a_i are non-negative, and $d_i \in \mathbb{R}$ $(i, j = 1, 2)$. The source terms are of the competitive Lotka-Volterra type

$$\tilde{F}_i(x, y, t, s_1, s_2) = \Big(\tilde{\alpha}_i(x, y, t) - \tilde{\beta}_{i1}(x, y, t)s_1 - \tilde{\beta}_{i2}(x, y, t)s_2\Big)s_i, \quad i = 1, 2, \ (7)$$

where $\tilde{\alpha}_i \geq 0$ is the intrinsic growth rate of the $i-$specie, $\tilde{\beta}_{ii} \geq 0$ are the coefficients of intra-specific competition, $\tilde{\beta}_{12},\ \tilde{\beta}_{21} \geq 0$ are those of inter-specific competition, and $s_i \in \mathbb{R}$. Function $U = U(x, y, t)$ is the environmental potential.

The above system of equations is completed with non-flux boundary conditions and initial data:

$$J_i \cdot \nu = 0 \quad \text{on} \quad \partial\Gamma_D \times (0, T), \tag{8}$$
$$u(\cdot, 0) = u_i^0 \quad \text{on} \quad \Gamma_D, \tag{9}$$

for $i = 1, 2$, where ν denotes the exterior unit normal to Γ_D.

We will refer to problem (6)-(9) for given U as to **Problem $\mathbf{P_S}$**. The first results on the existence of solutions of Problem $\mathrm{P_S}$ were proven under certain restrictions on the self and cross diffusion coefficients. For instance, for sufficiently small cross-diffusion terms (or small initial data) and vanishing self-diffusion coefficients $a_1 = a_2 = 0$, Deuring proved the global existence of solutions in [10]. For the case $c_1 = c_2$ a global existence result in one space dimension was obtained by Kim [21]. Furthermore, under the condition

$$2a_1 > 1, \quad 2a_2 > 1, \tag{10}$$

Yagi [34] showed the global existence of solutions in two space dimensions. A global existence result for weak solutions in any space dimension under assumption (10) can be found in [14]. Condition (10) can be easily understood by observing that in this case, the diffusion matrix is positive definite, hence yielding an elliptic operator. If the condition (10) does not hold, there are choices of $c_i,\ a_i,\ u_i \geq 0$ for which the diffusion matrix is not positive definite. In [15] the existence of global weak solutions for any $a_1,\ a_2 > 0$ was proven by using a suitable entropy functional. However, the proof uses the embedding $H^1(\Gamma_D) \subset L^\infty(\Gamma_D)$ in a crucial way such that the result is restricted to one space dimension only. Finally, the one-dimensional result was generalized by Chen and Jüngel [6] to three space dimensions without any restriction on the diffusion coefficients, although with additional assumptions on the Lotka-Volterra coefficients, see Hypothesys H_4 in Section 3. This result is fundamental for proving the existence of solutions of our model. We finally refer to [24,25] for the stationary problem, to [23,22] for other possibilities of Lotka-Volterra terms and notice that related models appear in chemotaxis and granular material theory [13,26,16].

2.2 Below the surface: salt and water relations in the porous medium

We assume the subsurface region, $\Omega \subset \mathbb{R}^3$, to be an open and bounded set that, after the introduction of dimensionless variables, see [12], takes the form $\Omega = \Gamma_D \times (0,1)$. We denote a point in Ω by $\mathbf{x} = (x, y, z)$, being z the depth. The subsurface is decomposed into a roots region, $\Omega_d = \Gamma_D \times (0, d)$, $d \in (0,1)$ where a continuous extraction of fresh water takes place, and a region free of roots, Ω/Ω_d.

In [12] we deduced the following dimensionless model. Let $c \in [0,1]$ be the salt concentration, $\mathbf{q}$ the water flow discharge and p the pressure, and consider the domain $Q_T = \Omega \times (0,T)$, for $T > 0$. Find $c, p : \bar{Q}_T \to \mathbb{R}$ and $\mathbf{q} : \bar{Q}_T \to \mathbb{R}^N$ such that

$$c_t + \mathrm{div}_{\mathbf{x}}(Rc\mathbf{q} - \nabla_{\mathbf{x}} c) = 0, \tag{11}$$
$$\mathrm{div}_{\mathbf{x}}\, \mathbf{q} + \tilde{g}(\cdot, c) = 0, \tag{12}$$
$$\mathbf{q} + \nabla_{\mathbf{x}} p + c\mathbf{e}_z = 0, \tag{13}$$

in Q_T. Here, $\mathrm{div}_{\mathbf{x}} = \frac{\partial}{\partial x} + \frac{\partial}{\partial y} + \frac{\partial}{\partial z}$, $\nabla_{\mathbf{x}} = (\frac{\partial}{\partial x}, \frac{\partial}{\partial y}, \frac{\partial}{\partial z})$ and the vector $\mathbf{e}_z$ is the canonical vertical vector pointing upwards. Positive parameter R is a Rayleigh number. The usual example considered in the literature [29,12] for the extraction function is of the form

$$\tilde{g}(z, c) = mk(z)(1-c)_+^r, \tag{14}$$

for $r > 0$, with $k(z) = d^{-1} 1_{(0,d)}(z)$ describing the localization of the roots, $d \in (0,1)$ and m, the extraction number, expressing the water uptaking strength, which is related to the mangroves *transpiration rate*. However, only general assumptions are needed to prove the existence of solutions, see [12], which read

$\tilde{\mathrm{H}}_2$. The function $\tilde{g} : \bar{Q}_T \times [0,1] \to \mathbb{R}$ satisfies

$\tilde{g} \in L^\infty(Q_T; C([0,1]))$,
$\tilde{g}(\mathbf{x}, t, \cdot)$ is non-increasing in $[0,1]$ and $\tilde{g}(\mathbf{x}, t, 1) = 0$ for a.e. $(\mathbf{x}, t) \in Q_T$.

In order to prescribe boundary conditions, we decompose the spatial boundary as $\partial\Omega = (\Gamma_D \times \{0\}) \cup \Gamma_N$, with $\Gamma_N = \Big(\Gamma_D \times \{1\}\Big) \cup \Big(\partial\Gamma_D \times (0,1)\Big)$. Here and it what follows, we make the identification $\Gamma_D \equiv \Gamma_D \times \{0\}$. We prescribe

$$c = c_D, \quad p = 0 \quad \text{on } \Gamma_D \times (0,T), \tag{15}$$
$$\nabla_{\mathbf{x}} c \cdot \mathbf{n} = \mathbf{q} \cdot \mathbf{n} = 0 \quad \text{on } \Gamma_N \times (0,T). \tag{16}$$

Finally, a non-negative initial distribution, c_0, is considered

$$c(\cdot, 0) = c_0 \quad \text{in } \Omega. \tag{17}$$

We will refer to the subsurface problem (11)-(17) as to **Problem $\mathbf{P_{SS}}$**.

As mentioned in the introduction, the first one-dimensional stationary version of this model was introduced by Passioura et al. [29]. It was later generalized in several ways but still keeping the one-dimensional space feature in van Duijn et al. [11], where several qualitative properties of the model were proven. Generalization to N space variables, tipically $N = 2, 3$, was introduced in van Duijn et al. [12], where the existence of solutions and stability issues were treated along with the numerical discretization of the problem. We shall use this existence result in a fundamental way. Finally, let us mention other two possibilities for extending the fluid model. One one hand, the extension of the physical domain to a two-regions model, water and porous medium, makes sense for the mangroves habitat, regularly inundated or actually waterlogged. To this respect, the Stokes-Darcy model would fit well with the physical problem, see [2,8] and the references therein. On the other hand, the consideration of a non-constant permeability tensor, embedded in our model as a constant in the Rayleigh number, would be also interesting, especially in the simplest case in which the tensor differs in the vertical and horizontal direction but is spatially uniform [33].

2.3 Coupling the surface and subsurface dynamics

Since in the present model we want to distinguish the features of both types of plant populations, we replace the extraction function of example (14), by

$$g = g_1 + g_2, \quad \text{with } g_i(z, c, u_1, u_2) = m_i k_i(z, u_1, u_2)(1 - c)_+^{r_i}, \quad i = 1, 2 \tag{18}$$

for the corresponding extraction numbers, m_i, and profiles of water uptaking, r_i, for each specie $i = 1, 2$. In addition, the presence of roots of specie i is represented by the function

$$k_i(z, u_1, u_2) = k(z)\frac{u_i}{u_1 + u_2},$$

in coincidence with that considered in [31]. We will see in the next section that the proof of existence of solutions of the general surface-subsurface problem requires weaker assumptions on g.

On the other hand, although the environmental potential in equation (6), U, is usually assumed to be given, in this model we will consider the case in which

it depends on the roots zone salt concentration in a way expressing that mangroves populations prefer to stablish in regions with low salt concentration. More concretely, we take

$$U(x,y,t) = \int_0^d c(x,y,z,t)dz, \tag{19}$$

where $d > 0$ is the roots region (constant) depth below the surface Γ_D, and c is the salt concentration of the solute which saturates the subsurface (porous medium). In addition, we will also assume that the Lotka-Volterra coefficients depend on the amount of water that each specie is able to extract (which depends on the salt concentration, c) and on other constant coefficients expressing that the species differ both in their ability to exclude salt and in other biological capabilities such as light or nutrients absortion, see [31]. Hence, for

$$G_i(x,y,t;c,u) = \int_0^1 g_i(z, c(\mathbf{x},t), u(x,y,t))dz \quad i = 1,2, \tag{20}$$

where we used the notation $u = (u_1, u_2)$, we define

$$F_i(x,y,t,u_1,u_2) = (\alpha_i - \beta_{i1}u_1 - \beta_{i2}u_2)u_i, \quad i = 1,2, \tag{21}$$

with,

$$\alpha_i = \alpha_i(G_i(x,y,t;c,u)), \quad \beta_{ij} = \beta_{ij}(G_1(x,y,t;c,u), G_2(x,y,t;c,u)), \tag{22}$$

for some functions $\alpha_i : \mathbb{R}_+ \to \mathbb{R}_+$ and $\beta_{ij} : \mathbb{R}_+^2 \to \mathbb{R}_+$.

The coupled surface-subsurface problem, which we will refer to as **Problem P**, is formed by the surface Problem $\mathrm{P_S}$ with the environmental potential given by (19) and the Lotka-Volterra coefficients given by (22), together with the subsurface Problem $\mathrm{P_{SS}}$ for an extraction function depending on the biomass u_1 and u_2, e.g. function g defined in (18).

3 Existence of solutions of the coupled problem

We assume the following hypothesis for proving the well-possednes of Problem P.

- $\mathrm{H_1}$. The spatial domain $\Omega \subset \mathbb{R}^N$, $N \leq 3$ is bounded with a Lipschitz continuous boundary, $\partial\Omega$, which is decomposed as $\partial\Omega = \Gamma_D \cup \Gamma_N$, with $\Gamma_D \cap \Gamma_N = \emptyset$ and with Γ_D of positive $N-1$ dimensional measure.
- $\mathrm{H_2}$. Let $\mathbf{x} = (x,y,z)$, $v = (v_1, v_2)$. The function $g : \bar{Q}_T \times [0,1] \times \mathbb{R}^2 \to \mathbb{R}$ satisfies, for $i = 1,2$,

$g(\cdot,\cdot,s,\cdot) \in L^\infty(Q_T \times \mathbb{R}^2)$ for all $s \in [0,1]$,
$g(\mathbf{x},t,\cdot,\cdot) \in C([0,1] \times \mathbb{R}^2)$ for a.e. $(\mathbf{x},t) \in Q_T$,
$g(\mathbf{x},t,\cdot,v)$ is non-increasing in $[0,1]$ and $g(\mathbf{x},t,1,v) = 0$ for a.e. $(\mathbf{x},t) \in Q_T$ and for all $v \in \mathbb{R}^2$.

Note that, in particular, $g \geq 0$ in $\bar{\Omega} \times [0,1] \times \mathbb{R}^2$.

H_3. The initial and boundary data have the regularity

$$
\begin{aligned}
&c_0 \in L^\infty(\Omega) \quad \text{and } 0 \leq c_0 \leq 1 \quad \text{a.e. in } \Omega,\\
&c_D \in H^1(0,T;L^2(\Omega)) \cap L^2(0,T;H^1(\Omega)) \quad \text{and } 0 \leq c_D \leq 1 \quad \text{a.e. in } Q_T,\\
&u_i^0 \in L_\Psi(\Gamma_D) \quad \text{and } u_i^0 \geq 0 \quad \text{a.e. in } \Gamma_D \ (i=1,2),
\end{aligned}
$$

with $L_\Psi(\Gamma_D)$ the Orlicz space for $\Psi(s) = (1+s)\ln(1+s) - s$, see [1].

H_4. The constant parameters satisfy $c_i \geq 0$, $a_i > 0$, $R \geq 0$, and $m \geq 0$. The Lotka-Volterra coefficients satisfy $\alpha_i \in C^0(\mathbb{R})$, $\beta_{ij} \in C^0(\mathbb{R}^2)$, with $\alpha_i \geq 0$, $\beta_{ii} > \beta > 0$, and $\beta_{12} = \beta_{21} \geq 0$, for $i,j = 1,2$ and some constant β.

Remark 1 *In [12], the time dependence of function $\tilde{g}$ we imposed in Hypothesis $\tilde{\mathrm{H}}_2$ was not considered. Analogously, the case of time-space dependent coefficients in the Lotka-Volterra function we assumed in (7) was not treated in [6]. However, these are minor changes which do not affect even to the notion of weak solution for Problems P_S and P_{SS}. A careful inspenction of the proofs in both articles shows that the conclusions of Theorem 1 of [12] and Theorem 1.1 of [6] remain valid under these more general assumptions.*

We finally introduce the usual concentration and flow-pressure functional spaces:

$$
\begin{aligned}
&\mathcal{V} = \left\{\eta \in H^1(\Omega) : \eta = 0 \text{ on } \Gamma_D\right\},\\
&H_{0,N}(\mathrm{div},\Omega) = \left\{\boldsymbol{\phi} \in L^2(\Omega)^N : \mathrm{div}_{\mathbf{x}}\, \boldsymbol{\phi} \in L^2(\Omega), \boldsymbol{\phi}\cdot\mathbf{n} = 0 \text{ on } \Gamma_N\right\},\\
&\mathcal{W}_T = \left\{\boldsymbol{\phi} \in L^2(Q_T)^N : \mathrm{div}_{\mathbf{x}}\, \boldsymbol{\phi} \in L^\infty(Q_T)\right\}.
\end{aligned}
$$

We have the following result.

Theorem 1 *Let $T > 0$ and assume Hypothesis H_1-H_4. Then Problem P has a weak solution $(u_1, u_2, c, \mathbf{q}, p)$ satisfying, for $i = 1,2$, the regularity*

$$u_i \in L^2(0,T;H^1(\Gamma_D)) \cap L^\infty(0,T;L_\Psi(\Gamma_D)) \cap W^{1,r}(0,T;(W^{1,r'}(\Gamma_D))'), \tag{23}$$

$$c \in c_D + L^2(0,T;\mathcal{V}) \cap H^1(0,T;\mathcal{V}') \cap L^\infty(Q_T), \tag{24}$$

$$\mathbf{q} \in L^2(0,T;H_{0,N}(\mathrm{div},\Omega)) \cap \mathcal{W}_T, \tag{25}$$

$$p \in L^2(0,T;\mathcal{V}), \tag{26}$$

for $r = (2N+2)/(2N+1)$ *and* $r' = r/(r-1)$, *and with*

$$u_i \geq 0 \quad \text{in } S_T \quad \text{and} \quad \min\{c_0, c_D\} \leq c \leq 1 \quad \text{in } Q_T.$$

Equations (6), (11)-(13) are satisfied in the sense

$$\begin{aligned}\int_0^T < \partial_t u_i, \varphi >_1 + \int_{S_T} (c_i \nabla u_i + 2a_i u_i \nabla u_i + \nabla(u_1 u_2) + d_i u_i \nabla U) \cdot \nabla \varphi \\ = \int_{S_T} F_i(\cdot, u_1, u_2)\varphi, \end{aligned} \tag{27}$$

for all $\varphi \in L^{r'}(0,T; W^{1,r'}(\Gamma_D))$, *and*

$$< c_t, \eta >_2 - \int_\Omega (Rc\mathbf{q} - \nabla_{\mathbf{x}} c) \cdot \nabla_{\mathbf{x}} \eta = 0, \tag{28}$$

$$\int_\Omega \mathbf{q} \cdot \boldsymbol{\phi} - \int_\Omega p \, \mathrm{div}_{\mathbf{x}} \boldsymbol{\phi} - \int_\Omega c \mathbf{e}_z \cdot \boldsymbol{\phi} = 0, \tag{29}$$

$$\int_\Omega (\mathrm{div}_{\mathbf{x}} \mathbf{q} + g(\cdot, c, u_1, u_2))\xi = 0, \tag{30}$$

for all $\eta \in \mathcal{V}$, $\xi \in L^2(\Omega)$, $\boldsymbol{\phi} \in H_{0,N}(\mathrm{div}, \Omega)$ *and for a.e.* $t \in (0,T)$. *The notation* $< \cdot, \cdot >_1$ *and* $< \cdot, \cdot >_2$ *stands for the dual products* $W^{1,r'}(\Gamma_D) \times (W^{1,r'}(\Gamma_D))'$ *and* $\mathcal{V}' \times \mathcal{V}$, *respectively. Finally, the initial data* $u_{i,0}$ *and* c_0 *are satisfied in the* L_Ψ *and* L^2 *senses, respectively.*

Proof. Since the coupling between Problems $\mathrm{P_S}$ and $\mathrm{P_{SS}}$ is weakly nonlinear, the proof of existence of solutions of Problem P is a direct application of the techniques used in the proofs of those problems, see [6,12]. Therefore, we will be schematic. The proof is based on the Schauder's fixed point theorem.

Definition of the fixed point operator. Let $\tilde{u} \in L^r(S_T)^2$, with $r = (N+2)/(N+1)$, be given and consider the extraction function $\tilde{g}(\mathbf{x}, t, s) = g(\mathbf{x}, t, s, \tilde{u}(x, y, t))$, with g a given function satisfying Hypothesis $\mathrm{H_2}$ implying that $\tilde{g}$ satisfies Hypothesis $\tilde{\mathrm{H}}_2$. Then, Theorem 1 of [12] enssures the existence of a weak solution, $(c, \mathbf{q}, p)$, of the subsurface Problem $\mathrm{P_{SS}}$ corresponding to $\tilde{g}$. We then consider the surface Problem $\mathrm{P_S}$ for U given by (19) and $\tilde{F}_i$ of the form (7), with the coefficients given by

$$\begin{aligned}\tilde{\alpha}_i(x,y,t) &= \alpha_i(G_i(x,y,t;c,\tilde{u})), \\ \tilde{\beta}_{ij}(x,y,t) &= \beta_{ij}(G_1(x,y,t;c,\tilde{u}), G_2(x,y,t;c,\tilde{u})),\end{aligned}$$

with α_i, β_{ij} satisfying Hypothesis $\mathrm{H_4}$, and with $G_i(x,y,t;c,\tilde{u})$ defined in (20). Since $c \in L^2(0,T;\mathcal{V})$ and $\tilde{u} \in L^r(S_T)^2$, we obtain $\nabla U \in L^2(S_T)$ and $\tilde{\alpha}_i$, $\tilde{\beta}_{ij}$, $i,j = 1,2$, satisfy the hypothesis of Theorem 1.1 of [6], from where we deduce

the existence of a weak solution $u \in L^r(S_T)^2$ of Problem $\mathrm{P_S}$. We consider the operator $\mathcal{G} : L^r(S_T)^2 \to L^r(S_T)^2$ given by

$$\mathcal{G}(\tilde{u}) = u, \tag{31}$$

and emphasize that a fixed point of $\mathcal{G}$ is a weak solution of Problem P.

The hypothesis of the fixed point theorem we have to check are: (i) $\mathcal{G}$ is continuous, (ii) $\mathcal{G}$ is compact, and (iii) the set

$$\Lambda = \{(\tilde{u}_1, \tilde{u}_2) \in L^r(S_T) \times L^r(S_T) : (\tilde{u}_1, \tilde{u}_2) = \lambda \mathcal{G}(\tilde{u}_1, \tilde{u}_2), \quad \text{for all } \lambda \in [0,1]\}$$

is bounded.

(i) $\mathcal{G}$ is continuous. Let $\tilde{u}_n \in L^r(S_T)^2$ be a sequence such that $\tilde{u}_n \to \tilde{u}$ strongly in $L^r(S_T)^2$ and set $u_n = \mathcal{G}(\tilde{u}_n)$ and $u = \mathcal{G}(\tilde{u})$. We have to check that $u_n \to u$ strongly in $L^r(S_T)^2$ as $n \to \infty$. As above, since $\tilde{u}_n \in L^r(S_T)^2$ Theorem 1 of [12] implies the existence of a weak solution $(c_n, \mathbf{q}_n, p_n)$ of the subsurface Problem $\mathrm{P_{SS}}$ corresponding to function $\tilde{g}_n(\mathbf{x}, t, s) = g(\mathbf{x}, t, s, \tilde{u}_n(\mathbf{x}, t))$ and satisfying (24)-(26) and (28)-(30). Using the uniform estimates obtained in the proof of Theorem 1 of [12] and taking into account that $\tilde{u}_n \to \tilde{u}$ strongly in $L^r(S_T)^2$, it is easy to prove that, up to a subsequence (not relabeled), we have $(c_n, \mathbf{q}_n, p_n) \to (c, \mathbf{q}, p)$, a weak solution of Problem $\mathrm{P_{SS}}$ corresponding to $\tilde{f}(\mathbf{x}, t, s) = f(\mathbf{x}, t, s, \tilde{u}(\mathbf{x}, t))$. We now solve Problem $\mathrm{P_S}$ for data related to c_n. Let

$$U_n(x, y, t) = \int_0^d c_n(x, y, z, t) dz,$$

and $\tilde{F}_i^n$ be given by (7) with the coefficients replaced by

$$\tilde{\alpha}_i^n(x, y, t) = \alpha_i(G_i(x, y, t, c_n, \tilde{u}_n)),$$
$$\tilde{\beta}_{ij}^n(x, y, t) = \beta_{ij}(G_1(x, y, t, c_n, \tilde{u}_n), G_2(x, y, t, c_n, \tilde{u}_n)).$$

The existence of a weak solution, u_n, of Problem $\mathrm{P_S}$ corresponding to U_n and $\tilde{F}_i^n$ and satisfying the regularity properties (23) and (27) is guaranteed by Theorem 1.1 of [6]. Next, we perform the limit $n \to \infty$ to this sequence of solutions of Problem $\mathrm{P_S}$. The only limits which are not already justified in the proof of Theorem 1.1 of [6] are

$$\int_{S_T} u_i^n \nabla U_n \cdot \nabla \varphi, \quad \text{and} \quad \int_{S_T} \tilde{F}_i^n(\cdot, u_n)\varphi. \tag{32}$$

The convergence of the first term is straightforward since, as shown in Lemma 3.4 of [6], $u_i^n \to u_i$ strongly in $L^2(S_T)$ and as shown in the proof of Theorem 1 of [12] $c_n \to c$ weakly in $L^2(Q_T)$, implying $\nabla U_n \to \nabla U$ weakly in $L^2(S_T)^2$, with

$$U(x, y, t) = \int_0^d c(x, y, z, t) dz.$$

For the second term of (32), we again use that $u^n \to u$ strongly in $L^2(S_T)^2$ and a.e. in S_T. In addition, we use that $c_n \to c$ strongly in $L^2(Q_T)$ (see [12]) and $\tilde{u}_n \to \tilde{u}$ strongly in $L^r(S_T)^2$. Then, since g_i is bounded and continuous with respect to the second and third variables, we have

$$G_i(x, y, t, c_n, \tilde{u}_n) \to G_i(x, y, t, c, \tilde{u})$$

strongly in $L^\gamma(S_T)$ for all $\gamma < \infty$. Using now the continuity of the Lotka-Volterra coefficients (Hypothesys H_4) we get $\tilde{\alpha}_i^n \to \tilde{\alpha}_i$ and $\tilde{\beta}_{ij}^n \to \tilde{\beta}_{ij}$ strongly in $L^\gamma(S_T)$, with

$$\tilde{\alpha}_i(x, y, t) = \alpha_i(G_i(x, y, t, c, \tilde{u})),$$
$$\tilde{\beta}_{ij}(x, y, t) = \beta_{ij}(G_1(x, y, t, c, \tilde{u}), G_2(x, y, t, c, \tilde{u})).$$

Finally, using the continuity of $\tilde{F}_i$ with respect to the last variable we obtain $\tilde{F}_i^n(x, y, t, u_n) \to \tilde{F}_i(x, y, t, u)$ strongly in $L^r(S_T)$. Therefore, with the convergence of both terms of (32) justified, we deduce $u_n \to u$ strongly in $L^r(S_T)^2$, and thus the continuity of $\mathcal{G}$.

(ii) $\mathcal{G}$ is compact. It is a consequence of the compact imbedding $L^r(S_T) \subset L^2(0, T; H^1(\Gamma_D)) \cap W^{1,r}(0, T; (W^{1,r'}(\Gamma_D))')$.

(iii) Λ is bounded. For $\lambda = 0$ is trivial. For $\lambda \in (0, 1]$ it is straightforward too. Condition $u = \lambda\mathcal{G}(u)$ is equivalent to $(u_1, u_2, c, \mathbf{q}, p)$ satisfying (27)-(29), and (30) replaced by

$$\int_\Omega (\mathrm{div}_{\mathbf{x}}\, \mathbf{q} + g(\cdot, c, u_1/\lambda, u_2/\lambda))\xi = 0, \tag{33}$$

for all $\xi \in L^2(\Omega)$ and for a.e. $t \in (0, T)$. Therefore, the only change estimating the $L^r(S_T)$ norm of u_i is in the right hand side term. But, since $\|g\|_{L^\infty}$ is uniformly bounded due to Hypothesis H_2, we may obtain similar estimates than those in the proof of Theorem 1.1 of [6], which imply the boundedness of Λ. □

4 Numerical experiments

In this section we present numerical simulations for the two dimensional problem which are based on a stabilized mixed finite element method for the subsurface problem and an explicit finite differences scheme for the surface problem. We start by introducing a time discretization of Problem P, i.e, we look for time independent functions u_1^k, u_2^k, c^k, q^k and p^k approximating the continuous solution u_1, u_2, c, q and p, respectively, in the time interval $(k\tau, (k+1)\tau]$,

for $k = 0, ..., N$, for some $N \in \mathbb{N}$ and $\tau = T/(N+1)$. Naturally, for $k = 0$ we set $u_1^0 = u_{10},\ u_2^0 = u_{20}$, etc.

For $t_k = k\tau$, let $u_1^{k-1},\ u_2^{k-1},\ c^{k-1},\ \mathbf{q}^{k-1}$ and p^{k-1} be given. We first compute $c^k,\ \mathbf{q}^k$ and p^k as a solution of a time discretized version of an equivalent formulation of Problem P_{SS}, consisting on combining equations (11) and (12) to replace (11) by

$$c_t + R\mathbf{q} \cdot \nabla c - \Delta c = Rcg(\cdot, c, \cdot, \cdot). \tag{34}$$

Time discretization. The time discrete problem corresponding to Problem P_{SS} is then formulated as

$$c^k + \tau(R\mathbf{q}^k \cdot \nabla c^k - \Delta c^k) = \tau R c^k g(\cdot, c^k, u_1^{k-1}, u_2^{k-1}) + c^{k-1}, \tag{35}$$
$$\operatorname{div} \mathbf{q}^k = -g(\cdot, c^k, u_1^{k-1}, u_2^{k-1}), \tag{36}$$
$$\mathbf{q}^k + \nabla p^k + c^k \mathbf{e}_z = 0, \tag{37}$$

in $\Omega = [0, L] \times [0, 1]$, with the boundary conditions

$$c^k = c_D, \quad p^k = 0 \quad \text{on } \Gamma_D, \tag{38}$$
$$\nabla c^k \cdot \mathbf{n} = \mathbf{q}^k \cdot \mathbf{n} = 0 \quad \text{on } \Gamma_N. \tag{39}$$

Once problem (35)-(39) is solved, we compute u_1^k, u_2^k as the solution of a time discretized version of problem P_S

$$u_i^k = u_i^{k-1} + \tau\Big(\Big(u_i^{k-1}(c_i + a_{i1}u_1^{k-1} + a_{i2}u_2^{k-1})\Big)_{xx} + \Big(d_i u_i^{k-1} U_x^k\Big)_x\Big), \tag{40}$$

in $[0, L]$, for $i = 1, 2$, where

$$U^k(\cdot) = \int_0^d c^k(\cdot, z)dz. \tag{41}$$

Observe that, without loss of generality, we again write Eq. (40) in not rescaled form, as Eq. (1). The non-flux boundary conditions are imposed by solving the system of equations for u_{1x}^k and u_{2x}^k given by

$$(c_1 + 2a_{11}u_1^{k-1} + a_{12}u_2^{k-1})u_{1x}^k + a_{12}u_1^{k-1}u_{2x}^k = -d_1 u_1^{k-1} U_x^k, \tag{42}$$
$$a_{21}u_2^{k-1}u_{1x}^k + (c_2 + 2a_{21}u_1^{k-1} + a_{22}u_2^{k-1})u_{2x}^k = -d_2 u_2^{k-1} U_x^k, \tag{43}$$

on $x = 0$ and $x = L$.

Space discretization. The space discretization of problem (35)-(39) is similar to that used in [12]. It is well known that classical mixed variational formulations

need an adequate election of the discrete spaces for the flow and the pressure in order to satisfy the Babuska-Brezzi stability condition, see for instance [5]. Following Masud and Huges [27], we consider a stabilized mixed finite element method for Darcy flows which allows to use piecewise linear approximations and the same mesh for both pressure and flow. For each discrete time t_k, we solve the nonlinear system of equations (35)-(39) by a fixed point method based on the proof of Theorem 1 of [12]. We consider the map $S : L^2(\Omega) \to L^2(\Omega)$ given by $S(\hat{c}; c^{k-1}) = c$, where c is the solution of

$$c - \tau\Delta c = -\tau R\mathbf{q} \cdot \nabla\hat{c} + \tau R\hat{c}g(\cdot, \hat{c}, u_1^{k-1}, u_2^{k-1}) + c^{k-1}, \tag{44}$$

$$\operatorname{div} \mathbf{q} = -g(\cdot, \hat{c}, u_1^{k-1}, u_2^{k-1}), \tag{45}$$

$$\mathbf{q} + \nabla p + \hat{c}\ \mathbf{e}_z = 0, \tag{46}$$

with the corresponding boundary conditions (38)-(39). A fixed point of $S(\cdot\,; c^{k-1})$ is denoted by c^k, and the corresponding velocity and pressure by $\mathbf{q}^k$ and p^k, respectively. To solve problem (44)-(46) for a given $\hat{c}$, we first solve problem (45)-(46), which has the following formulation in terms of the stabilized mixed finite element method: Find $\mathbf{q} \in H_{0,N}(\operatorname{div}, \Omega)$ and $p \in \mathcal{V}$ satisfying

$$\int_\Omega (\mathbf{q} + \nabla p) \cdot \boldsymbol{\phi} + \int_\Omega \hat{c}\ \mathbf{e}_z \cdot \boldsymbol{\phi} = 0 \quad \text{for all } \boldsymbol{\phi} \in H_{0,N}(\operatorname{div}, \Omega), \tag{47}$$

$$\int_\Omega (\nabla p - \mathbf{q}) \cdot \nabla\varphi + \int_\Omega (\hat{c}\ \mathbf{e}_z \cdot \nabla\varphi + 2g(\cdot, \hat{c}, u_1^{k-1}, u_2^{k-1})\varphi) = 0 \quad \text{for all } \varphi \in \mathcal{V}. \tag{48}$$

Once that $\mathbf{q}$ and p are determined, we set the following problem for equation (44): Find $c \in c_D + \mathcal{V}$ solution of

$$\int_\Omega c\varphi + \tau \int_\Omega \nabla c \cdot \nabla\varphi = \tau R \int_\Omega (\hat{c}g(\cdot, \hat{c}, u_1^{k-1}, u_2^{k-1}) - \mathbf{q} \cdot \nabla\hat{c})\varphi + \int_\Omega c^{k-1}\varphi, \tag{49}$$

for all $\varphi \in \mathcal{V}$. The spatial discretization for solving (47)-(48) is that given in [27], which we also adapt to equation (49). It consists of finite triangular elements, continuous piecewise linear basis functions with the same mesh for all the unknowns. For the practical implementation of the fixed point method, we construct a sequence $c_j^k = S(c_{j-1}^k; c^{k-1})$, with $c_0^k = c^{k-1}$ and consider that a discrete solution, c_j^k, of (47)-(49) is a fixed point of $S(\cdot\,; c^{k-1})$ if a suitable norm of $S(c_j^k; c^{k-1}) - c_j^k$, is smaller than a fixed tolerance, for some $j = 0, 1, \ldots$

Finally, for the spatial discretization of the one dimensional problem (40)-(43) we use a finite difference approximation whose nodes are the vertices of the triangles of the $2D$ mesh lying on the top boundary. The numerical convergence of this one-dimensional scheme was proven in [15]. Other numerical approaches to the cross-diffusion population problem were introduced more recently in the context of finite element methods ($N \leq 3$) by Barret and Blowey [4] and by a particle method ($N = 1$) by Gambino et al. [18]. However, for the 1D case, the results of the three methods seem to be rather similar.

Table 1
Parameter values common for all the experiments

Parameter	Symbol	Value
Diffusion coefficients	c_1, c_2	0
Cross diffusion coefficients	a_{ij}	0.1
Convection coefficients	d_1, d_2	$1, 40$
Rayleigh number	R	100
Extraction coefficients	m_1, m_2	$0.05, 0.1$
Extraction powers	r_1, r_2	$0.5, 2$
Roots depth	d	0.25

4.1 Experiments

We consider the spatial domain $\Omega = (0, 4) \times (0, 1)$, which is discretized by a triangular finite elements mesh containing 900 nodes. The top spatial boundary $\Gamma_D = (0, 4) \times \{0\}$ contains 30 nodes. The time step is selected considering the main time scales of the problem i.e., diffusion and convection. We take $dt = \min\{0.5\ dx^{-2}, (R\ dx)^{-1}\}$, with $dx = 1/30$. In some situations, for instance when large gradients of populations density arise, we interpolate the data of Problem P_S to a finer mesh on Γ_D in order to get a smoother approximation. The data on Table 1 is common for all the experiments. Observe that the linear diffusions are set to zero, and that the cross-diffusion coefficients have the same value, indicating that population pressures affect in a similar way to both species. The differences between the biological characteristics of the species (mangroves represented by u_1 and a less salt tolerant specie represented by u_2) are captured by (i) the convection coefficients, $d_1 \ll d_2$, indicating a bigger atraction of Specie 2 than mangroves towards the low salinity areas, and (ii) the coefficients appearing in the extraction function, g, i.e., the extraction numbers, $m_1 < m_2$, indicating a more efficient behaviour of Specie 2 for extracting water when no salt is present, and $r_1 < 1 < r_2$, implying a larger capacity of mangroves to uptake fresh water from saline waters. Since we take a relatively low Rayleigh number we do not expect neither large gradients of the salt concentration nor important variations of the flow in the subsurface. However, the situation changes on the surface due to the powerfull combination of the drift effects produced by the environmental potential and the repulsive effects of the cross-diffusion. This combination results on large gradients of the populations density in the "good" environmental regions.

Experiment 1. We test the model in a standard situation. We take the salt concentration data as $c_0 = c_D = 0.5$, and initial population distributions which contain areas where the species are isolated and areas where the species share

the space with equal population density, see Fig. 1. We set the Lotka-Volterra terms to zero, implying for the continuous model that the populations mass have to be conserved. Indeeed, for the discrete model, recalling that the time discretization scheme is explicit, the mass conservation property is quite well captured, having a relative error of the order of 10^{-5}. More precisely, for the stopping time $T = 80$ years (dimensional model), we have

$$\max_{i=1,2}\left\{\Big(\int_0^4 u_{i0}(x)dx - \int_0^4 u_i(x,T)dx\Big)\Big(\int_0^4 u_{i0}(x,t)dx\Big)^{-1}\right\} = 1.3794\times 10^{-5}.$$

In Fig. 1 we show the initial and final population density distributions for both species. Since the initial salt concentration distribution is homogeneous, the environmental potential is initially not attracting the populations to a definite place. However, as time evolves, mangroves salinize the region they occupy, creating a gradient on the environmental potential which drives the population of Specie 2 energically ($40 = d_2 \gg d_1 = 1$) towards the potential minimum. Fig. 2 shows the population distributions evolution by plotting $u_i(x,t)$ for $t = 0,\ 15,\ 30,\ 45,\ 60,\ 80$ years. In Figs. 3 and 4 we show some aspects of the concentration-flow problem in the porous medium: the evolution of the environmental potential (same time slices than above), given by

$$U(x,t) = \int_0^{0.25} c(x,z,t)dz,$$

the water flow, and two time slices of the salt concentration. Observe that the absolute changes of the environmental potential are very small, but enough to induce the populations segregation.

Experiment 2. We use the same initial population distributions than in Experiment 1 but assume an initial and boundary salt concentration which increases with x, simulating a usual situation in the mangroves habitats near the shore, see Fig. 6, left. We again set the Lotka-Volterra terms to zero. We run the program till $T = 80$ years and check that the relative error for the populations mass conservation is of the order 10^{-16}. In Fig. 5 we show the population distributions evolution by plotting $u_i(x,t)$ for $t = 0,\ 15,\ 30,\ 45,\ 60,\ 80$ years. The drift effect is notorious for Specie 2. In Fig. 6, right, we plot the salt concentration distribution for $T = 80$ years and $z = 0,\ 0.25,\ 1$, i.e., on the surface, at the lower limit of the roots region, and on the bottom. We observe that, although increasing faster than in other regions, the boundary $x = 0$ keeps being an attraction point region (lower salt concentration) where population of Specie 2 tends to concentrate.

In the following two experiments we explore the effects of the competition terms. We take initial population distributions constant and equal, $u_{10} = u_{20} = 0.5$, and keep the initial salt concentration as in Experiment 2.

Experiment 3. We consider two sets of Lotka-Volterra terms in order to

compare the evolution of population densities for fixed and varying growth and competition coefficients. More explicitly, we take, for $i = 1, 2$,

$$F_1(x,t) = G_1(x,t)\Big(300 - 100u_1(x,t) - 50u_2(x,t)\Big)u_1(x,t),$$
$$F_2(x,t) = G_2(x,t)\Big(300 - 50u_1(x,t) - 100u_2(x,t)\Big)u_2(x,t),$$

with G_i given by

$$G_i(x,t) = m_i \frac{u_i(x,t)}{u_1(x,t) + u_2(x,t)} \int_0^d (1 - c(x,z,t))_+^{r_i} dz,$$

and similar functions $\tilde{F}_i$ with $G_i(x,t)$ replaced by the constant value

$$\tilde{G}_i = \frac{1}{4}\int_0^4 G_i(x,0)dx.$$

We denote by $\tilde{u}_i$ the solutions corresponding to $\tilde{F}_i$ (Problem $\tilde{\text{P}}$) . We observe that, although the Lotka-Volterra coefficients would give a coexistence state for the corresponding dynamical system, in both cases (Problems P and $\tilde{\text{P}}$) the system seems to converge to the extinction of Specie2, $u_2 = \tilde{u}_2 = 0$, and to the equilibrium value $u_1 = \tilde{u}_1 = 3$ for the mangroves population. However, although qualitatively similar, the solutions of both problems have important quantitative differences. In Fig. 7, left, we plot the relative differences $\|u_i - \tilde{u}_i\|_{L^2(\Gamma_D)}\|\tilde{u}_i\|^{-1}_{L^2(\Gamma_D)}$. The magnitude of the difference is well explained by the time evolution of the coefficients of Problem P, which are captured by the extraction functions G_i, in comparison with the constant coefficients of Problem $\tilde{\text{P}}$. We plot in Fig. 7, center, the space average of these functions, i.e.,

$$\frac{1}{4}\int_0^4 G_i(x,t)dx.$$

Another visualization of the quantitative differences between the tho sets of solutions is given in Fig. 7, right, where we plot the space averaged mass populations

$$U_i(t) = \frac{1}{4}\int_0^4 u_i(x,t)dx, \quad \tilde{U}_i(t) = \frac{1}{4}\int_0^4 \tilde{u}_i(x,t)dx,$$

and the semi-total mass populations $(U_1 + U_2)/2$, and $(\tilde{U}_1 + \tilde{U}_2)/2$. We see that after a transient state of about one hundred years, both systems enter in a phase of slow increase (decrease) of the mass of mangroves (Specie2). However, the quantitative differences between both problems are significant. Mangrove (Specie 2) population is always larger (smaller) for Problem P than for Problem $\tilde{\text{P}}$. We also observe that the mass of Specie 2 corresponding to the constant coefficients, $\tilde{u}_2$, is always above the initial mass, whereas the same quantity for the variable coefficients problem drops below the initial state after

some 150 years. It is also interesting to notice that the total mass is practically constant for both problems, after the transient state.

Finally, in Fig. 8 we plot time slices showing the evolution of the populations distributions for problems P and $\tilde{\mathrm{P}}$. We see that after a fast initial growth of Specie 2, its population declines and tends to disappear from the *bad* environmental region. This effect is specially visible for solutions of Problem P. In fact, the competition between both populations seems to be more extreme in the case of variable coefficients, as may be seen in the *good* region boundary $x = 0$. The evolution of the system seems to lead to the semi-trivial steady state $(u_1, u_2) = (3, 0)$, i.e. extinction of Specie 2.

References

[1] R. A. Adams, Sobolev Spaces, Academic Press, New York, 1975.

[2] P. Angot, On the well-posed coupling between free fluid and porous viscous flows, Applied Mathematics Letters 24(2011) 803-810.

[3] M. C. Ball, Salinity tolerance in the mangroves *Aegiceras corniculatum* and *Avicennia marina*. I. Water use in relation to growth, carbon partitioning and salt balance, Aust. J. Plant Physiol. 15 (1988) 447-464.

[4] J. W. Barrett, J. F. Blowey, Finite element approximation of a nonlinear cross-diffusion population model, Numer. Math. 98 (2004) 195221.

[5] F. Brezzi, M. Fortin, Mixed and hybrid finite element methods, Springer Series in Computational Mathematics, 15, Springer-Verlag, New York, 1991.

[6] L. Chen, A. Jüngel, Analysis of a multidimensional parabolic population model with strong cross-diffusion, SIAM J. Math. Anal. 36(1) (2004), 301–322.

[7] X. Chen, R. Hambrock, Y. Lou, Evolution of conditional dispersal: a reaction-diffusion-advection model, J. Math. Biol. 57 (2008) 361-386.

[8] M.R. Correa, A.F.D. Loula, A unified mixed formulation naturally coupling Stokes and Darcy flows, Comput. Methods Appl. Mech. Engrg. 198 (2009) 2710-2722.

[9] C. Cosner, Y. Lou, Does movement toward better environments always benefit a population?, J. Math. Anal. Appl. 277 (2003) 489-503.

[10] P. Deuring, An initial-boundary value problem for a certain density-dependent diffusion system, Math. Z. 194 (1987), 375-396.

[11] C. J. van Duijn, G. Galiano, M. A. Peletier, A diffusion-convection problem with drainage arising in the ecology of mangroves, Interfaces and Free Boundaries 3 (2001) 15-44.

[12] C. J. van Duijn, G. Galiano, J. Velasco, Existence of solutions and stability analysis for a Darcy flow with extraction. Nonlinear Analalysis RWA 10(4) (2009) 2007-2020.

[13] H. Gajewski, K. Zacharias, Global behaviour of a reaction-diffusion system modelling chemotaxis, Math. Nachr. 195 (1998), 77-114.

[14] G. Galiano, M. L. Garzón, A. Jüngel, Analysis and numerical solution of a nonlinear cross-diffusion system arising in population dynamics, RACSAM Rev. R. Acad. Cienc. Exactas Fs. Nat. Ser. A Mat. 95(2) (2001), 281-295

[15] G. Galiano, M. L. Garzón, A. Jüngel, Semi-discretization in time and numerical convergence of solutions of a nonlinear cross-diffusion population model, Numer. Math. 93(4) (2003) 655-673.

[16] G. Galiano, A. Jüngel, J. Velasco, A parabolic cross-diffusion system for granular materials, SIAM J. Math. Anal. 35(3) (2003), 561-578

[17] G. Galiano, J. Velasco, On a dynamical boundary value problem arising in the ecology of mangroves. Nonlinear Analysis RWA 7(5) (2006) 1129-1144.

[18] G. Gambino, M.C. Lombardo, M. Sammartino, A velocitydiffusion method for a LotkaVolterra system with nonlinear cross and self-diffusion, Applied Numerical Mathematics 59 (2009) 1059-1074.

[19] R. Hambrock, Y. Lou, The Evolution of Conditional Dispersal Strategies in Spatially Heterogeneous Habitats, Bulletin of Mathematical Biology 71 (2009) 1793-1817.

[20] P. Hutchings, P. Saenger, Ecology of mangroves, Queensland, University of Queensland Press, 1987.

[21] J.U. Kim, Smooth solutions to a quasi-linear system of diffusion equations for a certain population model, Nonlinear Analysis TMA 8 (1984), 1121-1144.

[22] I. Kusbeyzi, O.O. Aybar, A. Hacinliyan, Stability and bifurcation in two species predator-prey models, Nonlinear Analysis RWA 12 (2011) 377-387.

[23] X. Liu, M. Han, Chaos and Hopf bifurcation analysis for a two species predator-prey system with prey refuge and diffusion, Nonlinear Analysis RWA 12 (2011) 1047-1061.

[24] Y. Lou, W.-M. Ni, Diffusion, self-diffusion and cross-diffusion, J. Diff. Eqs. 131 (1996), 79-131.

[25] Y. Lou, W.-M. Ni, Y. Wu, The global existence of solutions for a cross-diffusion system, Adv. Math., Beijing 25 (1996), 283-284.

[26] A. Marrocco, Numerical simulation of chemotactic bacteria aggregation via mixed finite elements, Math. Mod. Numer. Anal. 37 (2003), 617-630.

[27] A. Masud, T. Huges, A stabilized mixed finite element method for Darcy flow, Computer methods in applied mechanics and engineering 191 (2002), 4341-4370.

[28] M. Mimura, K. Kawasaki, Spatial segregation in competitive interaction-diffusion equations, J. Math. Biol. 9 (1980) 49-64.

[29] J. B. Passioura, M. C Ball, J. H. Knight, Mangroves may salinize the soil and in so doing limit their transpiration rate, Funct. Ecol. 6 (1992) 476-481.

[30] N. Shigesada, K. Kawasaki, E. Teramoto, Spatial segregation of interacting species, J. Theor. Biol. 79 (1979), 83-99.

[31] S. Y. Teh, D. L. DeAngelis, L. S. Lobo Sternberg, F. R. Miralles-Wilheim, T. J. Smith, H. L. Koh, A simulation model for projecting changes in salinity concentrations and species dominance in the coastal margin habitats of the Everglades, Ecological Modelling 213 (2008) 245-256.

[32] P. B. Tomlinson, The Botany of Mangroves, Cambridge University Press, Cambridge, U.K., 1986.

[33] X. Xu, S. Chen, D. Zhang, Convective stability analysis of the long term storage of carbon dioxide in deep saline aquifers, Advances in Water Resources 29 (2006) 397-407.

[34] A. Yagi, Global solution to some quasilinear parabolic system in population dynamics, Nonlinear Analysis TMA 21 (1993), 603-630.

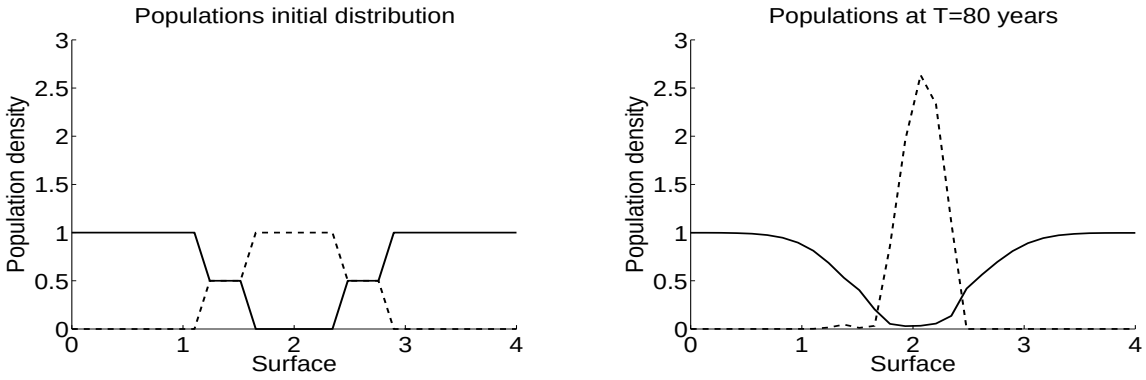

Fig. 1. Experiment 1. Continuous line: mangroves. Dotted line: Specie 2.

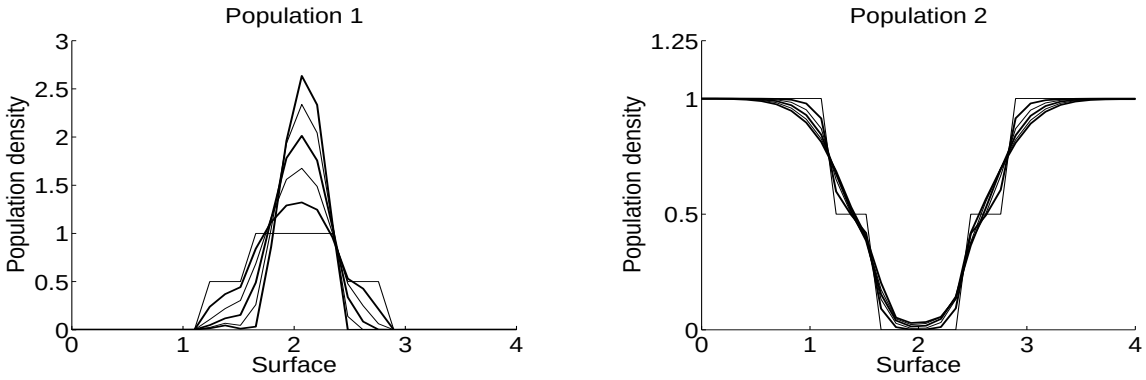

Fig. 2. Experiment 1. Time slices of the evolution of Specie 2 (left) and mangroves (right).

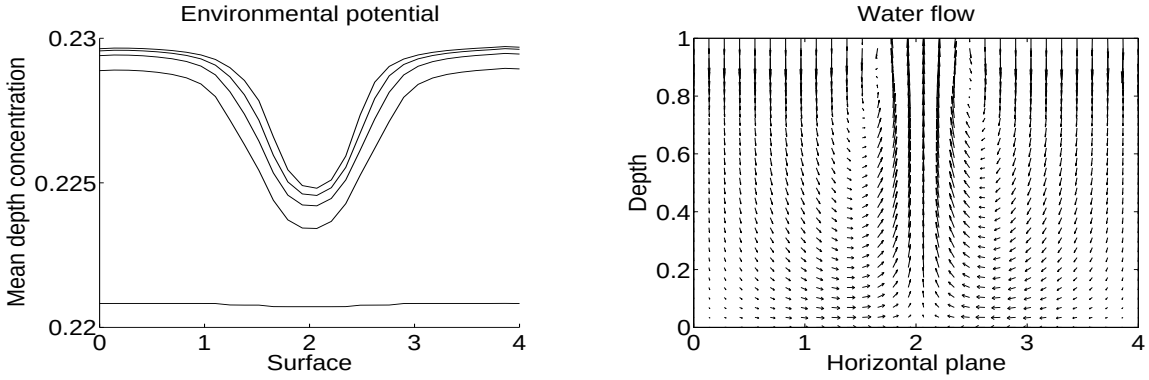

(a) Time slices of the evolution of the environmental potential.

(b) Water flow in the porous medium for T=80 years.

Fig. 3. Experiment 1. In the subsurface.

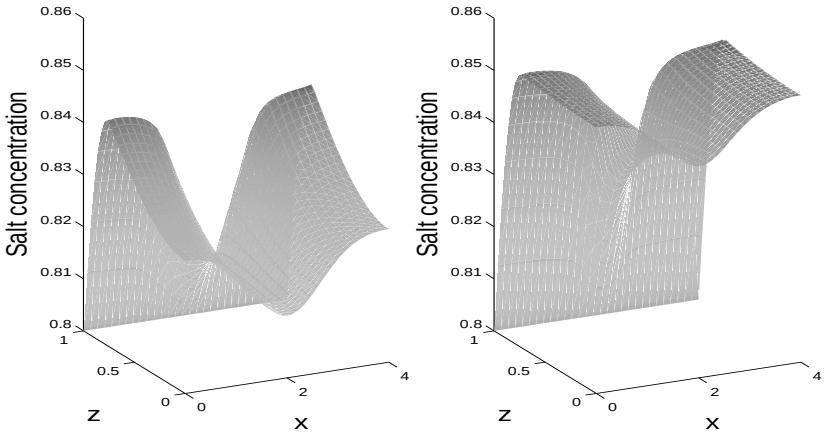

Fig. 4. Experiment 1. Salt concentration in the porous medium for T=10 years (left) and T=80 years (right). $z = 1$ corresponds to the top boundary Γ_D.

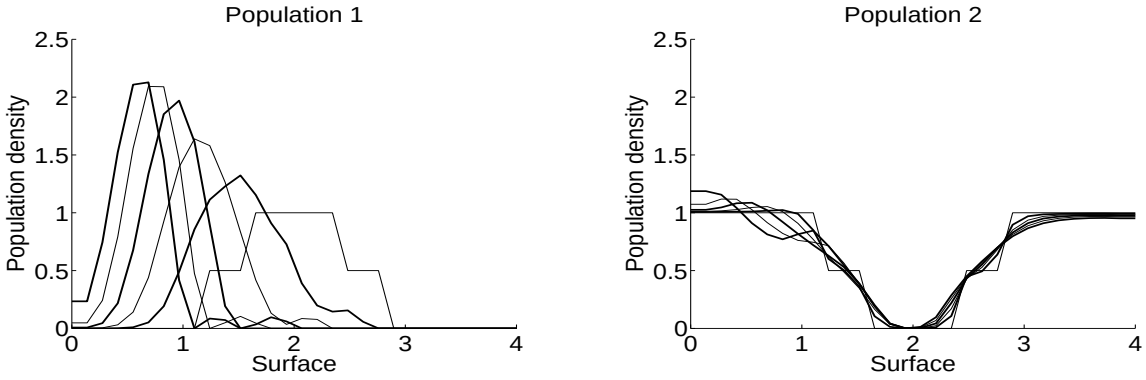

Fig. 5. Experiment 2. Time slices of the evolution of Specie 2 (left) and mangroves (right).

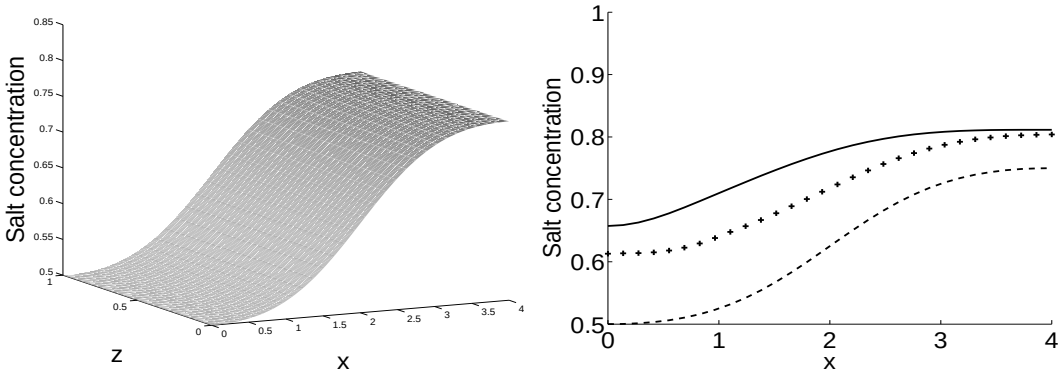

Fig. 6. Experiment 2. Salt concentration in the soil. Left: for $T = 0$. Right: for $T = 80$ years and at the bottom, $z = 1$, (continuous line), lower limit of the roots region, $z = 0.25$, (crossed line) and surface $z = 0$ (dotted line).

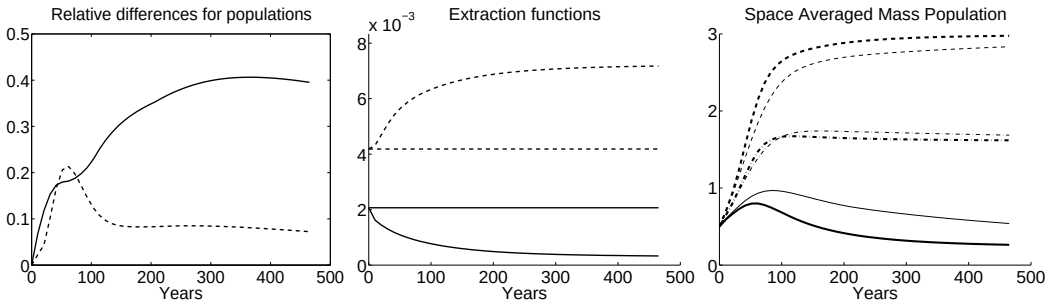

Fig. 7. Experiment 3. Several visualizations of the differences among solutions of Problems P and $\tilde{\text{P}}$. Mangroves: dotted lines, Specie 2: continuous lines.

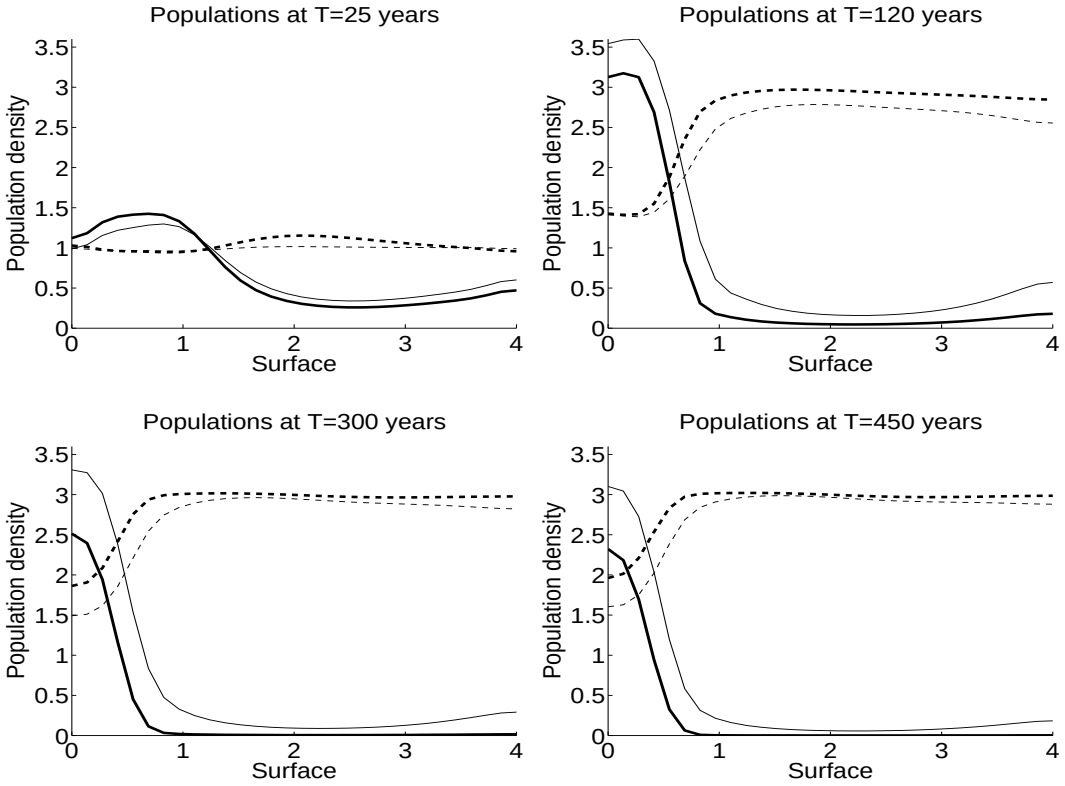

Fig. 8. Experiment 3. Populations evolution. Mangroves: dotted lines, Specie 2: continuous lines. Problem P: thick lines. Problem $\tilde{\text{P}}$: thin lines.